

Final Draft
of the original manuscript:

Uz, M.-V.; Kocak, M.; Lemaitre, F.; Ehrstroem, J.-E.; Kempa, S.; Bron, F.:
**Improvement of damage tolerance of laser beam welded stiffened
panels for airframes via local engineering**
In: International Journal of Fatigue (2008) Elsevier

DOI: 10.1016/j.ijfatigue.2008.10.003

IMPROVEMENT OF DAMAGE TOLERANCE OF LASER BEAM WELDED STIFFENED PANELS FOR AIRFRAMES VIA LOCAL ENGINEERING

M.-V. Uz¹, M. Koçak¹, F. Lemaitre², J.-C. Ehrström², S. Kempa³, F. Bron²

¹ GKSS Research Center, Institute of Materials Research
Materials Mechanics Section, Dept. of Joining and Assessment,
D-21502, Geesthacht, Germany

² ALCAN Centre de Recherches de Voreppe (CRV) Aerospace
Technical Products, Voreppe Cedex, France

³ ALCAN Technology & Management Ltd.
Multimaterial Surface & Joining, Neuhausen, Switzerland

Abstract

Damage tolerance of aerospace grade aluminum alloys was studied in relation to a new design philosophy in skin and stringer geometries. Systematic thickness variations (crenellations) were introduced onto the skin and stringers of the laser beam welded (LBW) stiffened Al2139-T8 large flat panels in order to modify the stress intensity factor (SIF) distribution on center cracked panels in such a way that fatigue life can be improved. Fatigue crack propagation (FCP) tests (on panels with crenellations) with crack growing perpendicular to the welded stringers were conducted under constant amplitude and spectrum loading conditions. Results were compared with the results of “classical” LBW stiffened panels (with no crenellations) having equal weight and tested under the same conditions. The new panel design with crenellations showed substantially longer fatigue lives under constant amplitude loading. This gain significantly improved under spectrum (Mini-Twist) loading fatigue tests. This paper presents the first FCP test results of a comprehensive ongoing program which investigates the benefits and potential role of crenellations on welded Al-alloy and steel structures. Further issues including microstructural examinations, numerical investigations, fitness for service analysis and residual strength aspects will be topics of another communication.

Keywords: Damage tolerance; fatigue life improvement; stiffened panels; crenellations; laser beam welding

1. Introduction

The current metallic aircraft manufacturing technology is in a highly saturated level and it is rather challenging to obtain significant weight and manufacturing cost savings without introduction of radical changes on the current design & fabrication routes and materials. Such a development was experienced in the recent years by application of laser beam welding (LBW) process for the skin-stringer joints of airframes. This technology offers significant weight and cost savings over the conventional riveting technique. Currently this technology is used for the lower fuselage panels, where the damage tolerance requirements of the structure are relatively less stringent. In this context, new design and manufacturing methodologies

which can give rise to significant improvements in the damage tolerance of metallic airframe components may bring two fold advantages. That is, new concepts offering higher damage tolerance not only enable producers to use thinner sheets for manufacturing, but also it may become possible to take the advantage of LBW technology on the more severely loaded sections of the fuselage.

For an improvement in damage tolerance of structures, two basic methodologies exist. First, the damage tolerance properties of the material can be improved (higher inherent crack resistance) and, second, the design of the structures can be modified to provide crack retardation, turning or arrest. In this joint research program of ALCAN and GKSS, both methodologies were utilized concurrently. That is, a newly developed, high strength, high toughness aluminum alloy was used in conjunction with a new skin and stringer design concept (containing “crenellations”) to obtain improved damage tolerance properties.

1.1. Crenellations, A New Concept

In order to improve the damage tolerance of the stiffened panels, crenellations (thickness variations) were introduced onto the skin sheets and stringers (Figure 1). It should be noted that, crenellations are not integral crack arresters already being used in aerospace industry. Crack arresters add some extra weight onto the structures. However, crenellations used in this study, do not lead to weight increase as the extra weight of the thicker skin regions principally compensated by the thickness reduction of thinner parts. Hence, the overall weight of the crenellated panel is equal to that of smooth (non-crenellated) reference panel. As it will be demonstrated, this new panel design improves the fatigue crack propagation resistance in direction perpendicular to crenellations. This preferentially strengthened direction then can be aligned with the highly loaded direction of the specific section of an airframe. In other words, considering that in certain sections of an airframe there exist differences in severity of loading in longitudinal and transverse directions (eg. upper fuselage, where the longitudinal bending of the fuselage imposes additional tension in the direction parallel stringers), the damage tolerance of the component can also be tailored to respond this loading condition in a more effective way.

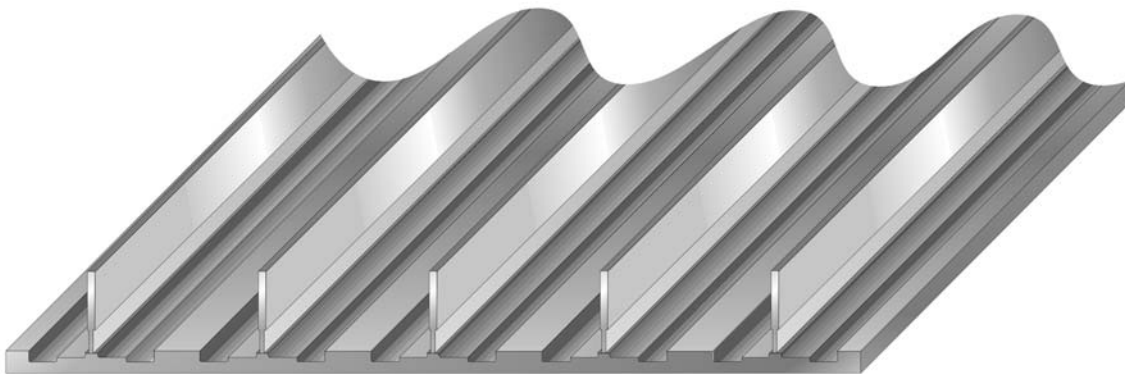


Figure 1: Schematic representation of a crenellated test panel. Note to the thickness variations both in skin and stringers. For simplification of the geometry, L-shaped stringers were not used.

The principal mechanism of the role of the crenellations on FCP can be described as follows: Consider, a cracked metallic component where FCP behavior can be described by Paris Law,

$\frac{da}{dN} = C\Delta K^m$. This component operates under cyclic far field loading of constant amplitude

which creates a certain stress intensity factor (SIF) range ΔK_a at the crack tip. If this SIF range can be increased for the half of the crack length and reduced with the same factor at the

remaining half, it seems that it is possible to obtain an extension in the fatigue life of the component compared to case where the crack is driven through the entire crack length by the original SIF range, ΔK_a . The form of the Paris equation offer that, when the FCP rate increased and decreased by modification of SIF range with a constant ratio, the fatigue life gain in the slow growth region will be higher than the life shortening in the fast growth region. For example, according to Paris Law, life of a crack driven by a SIF range of ΔK_a over a small crack extension length of $2\Delta a$ can be calculated as:

$$N_{ref} = \frac{2\Delta a}{C\Delta K_a^m} \quad (1)$$

with the assumption that the length $2\Delta a$ is short enough that the increase in the SIF resulting from the increase in crack length can be neglected.

For the same crack, if it is possible to reduce ΔK_a by a factor, t , for the half of propagation length and increase it with the same factor for the other half of the propagation, neglecting any possible loading history effects, modified fatigue lifetime becomes:

$$N_{mod} = \frac{\Delta a}{C(\Delta K_a - t\Delta K_a)^m} + \frac{\Delta a}{C(\Delta K_a + t\Delta K_a)^m} \quad (2)$$

It can be easily shown that, for any value of t in the interval (0, 1),

$$N_{mod} > N_{ref} \quad (\text{Details given in Appendix 1}) \quad (3)$$

In other words, it can be proved that the modified fatigue life, N_{mod} , of the component is longer than the original fatigue life, N_{ref} , for any value of t between 0 and 1. When the form of the inequality examined (Appendix 1), it can be realized that with increasing Paris exponent m and modification factor t , the enhancement in fatigue life increases.

Numerical SIF calculations showed that, the shape of the stress intensity factor distribution resulted from the introduction of crenellations is rather complex compared to the simplified step function assumption of above explained approach (Figure 2). Additionally, it was seen that higher thickness steps give larger fluctuations in SIF values which would result in larger fluctuations in SIF ranges (and longer lives) under cyclic loading.

In addition to SIF range, maximum (or mean) SIF value has an important affect on the FCP behavior of the metals, which is generally incorporated in fatigue life calculations through R-ratio [1, 2]. Therefore, such a modification of SIF profile affects the FCP rate not only through SIF range but also through SIF_{max} values.

After numerical evaluations, the methodology was first tried on integrally machined thick plates for which main target area can be, for example, wing applications [3]. The current study was set to conduct systematic investigation to describe the effect of crenellations on the damage tolerance behavior of the Al-alloy panels containing laser beam welded stringers for fuselage applications. This paper aims to report first results of the on-going investigations.

2. Experimental Procedure

2.1. Methodology and Approach

In order to examine the effect of crenellations on FCP behavior, constant amplitude and spectrum loading fatigue tests were conducted on large panels containing 5 LBW stringers.

Results were compared with reference specimens having equal weight and tested under the same conditions.

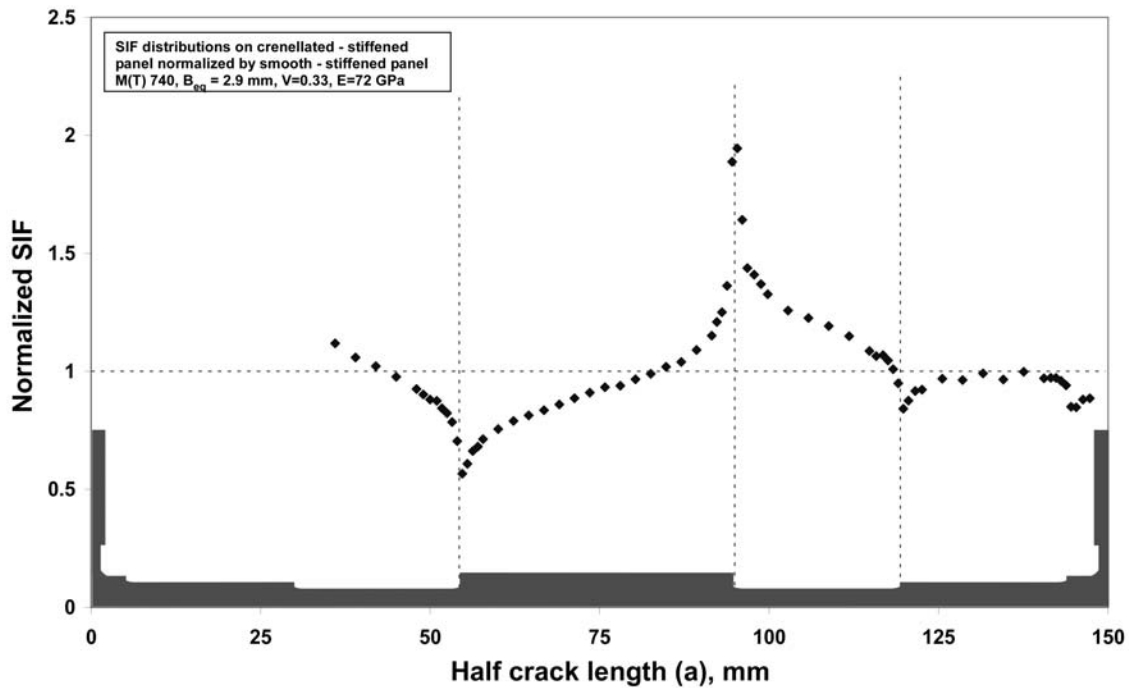


Figure 2: SIF profile of a center through crack on a crenellated stiffened panel for lengths from $a=37$ mm to $a=148$ mm. Values normalized by SIF values of reference panel (See Figure 3)

During the design stage of the crenellated panels, the main aim was creating a LBW stiffened panel having higher FCP resistance in one direction (direction transverse to crenellations) compared to a reference LBW stiffened panel having the same weight and outer dimensions. Additionally, only limited amount of reduction in damage tolerance properties in the direction parallel to the crenellations was aimed.

A 2.9 mm thick (non-crenellated), LBW stiffened specimen with 5 stringers, representing currently used fuselage panels was designed (Figure 3-a) as reference panel. The stringer pitch in this panel was 150 mm, panel width ($2W$) was 740 mm and panel length was 1200 mm. Then, a crenellated panel with the same outer dimensions was designed based on several criteria. Not to complicate non-destructive testing issues in a potential application, crenellation sections kept at least 25 mm wide (Figure 3-b). Only the pad-up under the stringers were 10 mm wide as keeping this width smaller is critical in terms damage tolerance of weld line cracks. The thinnest region of the crenellation pattern was 1.9 mm thick, which corresponds to some 35% reduction from the reference thickness of 2.9 mm. Considering the loading differences between longitudinal and transverse directions in the potential application regions of the fuselage and the improved damage tolerance of the 2139-T8 material compared to the conventional high damage tolerance aluminum alloys, such a reduction was thought to be reasonable. The crenellation profile contained a steep step (1.9 to 4.15 mm) and repeated itself in each bay. The edges of crenellations rounded with a radius of curvature of 1 to 1.5 mm.

45 mm high straight-shaped stringers were used instead of commonly used L formed ones to simplify specimen preparation. One single step of 2 mm height was introduced onto the

stringers at a distance of 10 mm from the lower end (Figure 3). Thickness of the lower part was 2.5 mm and the rest was 4.5 mm (single stringer crenellation!). In addition to constituting an effective crack retardation site, this step step facilitated the welding process by reducing the necessary heat input for welding. Lower heat input (because of lower necessary weld metal volume) facilitates controlling the distortion. Identical stringer geometry was used also for reference panels (Figure 3-a). A photo of one of the crenellated panels is shown in Figure 4.

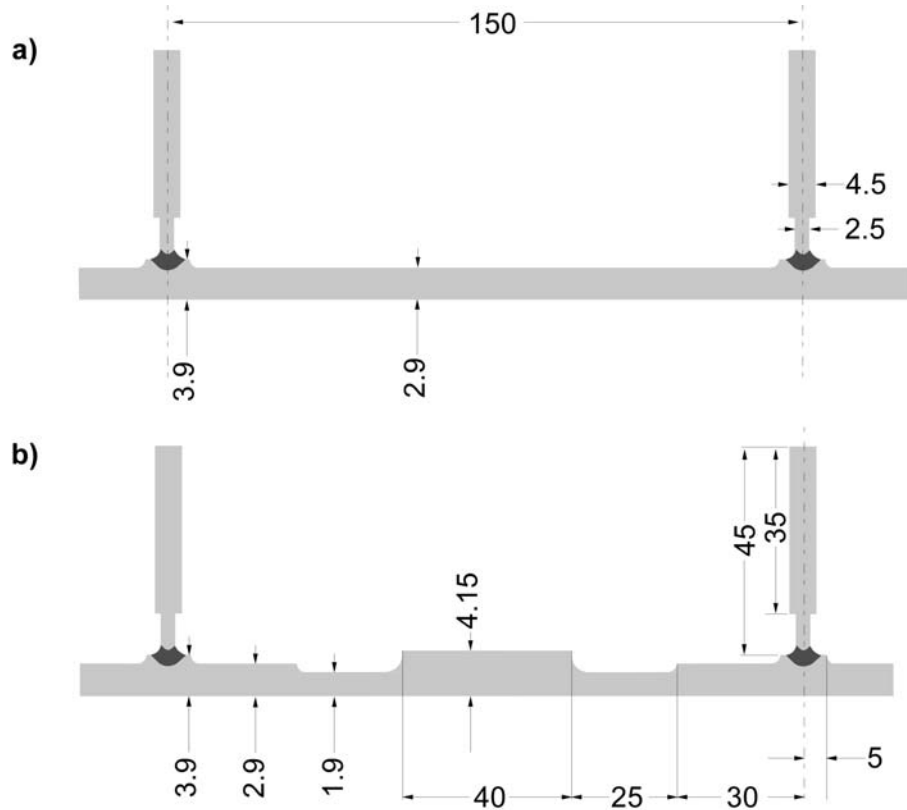


Figure 3: Schematic representation of a) Reference geometry, b) Crenellated geometry

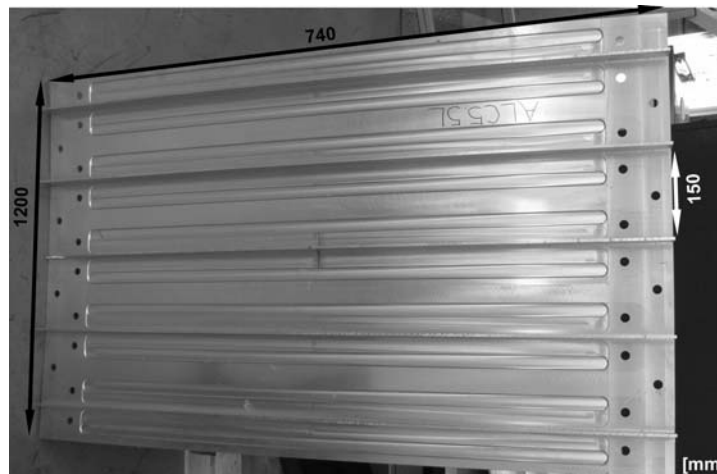


Figure 4: General view and dimensions of crenellated panel

2.2. Preparation of Test Panels

Both crenellated and reference panels were machined from 4.5 mm thick Al2139 sheets in T3 heat treatment condition. By machining, thickness in the middle 1000 mm of the reference panels was reduced to 2.9 mm. During this process, five 10 mm wide sockets were left with a thickness of 3.9 mm. In a similar manner, crenellation pattern was introduced in the middle 1000 mm region of crenellated specimens by machining. At this stage, panel length was 1300 mm. The thickness of the 150 mm long sections at both ends was kept 3.9 mm in order to reinforce the loading ends. Stringers were also machined from the same 4.5 mm thick 2139-T3 sheets.

Welding process was conducted using an Nd:YAG laser beam source. Stringers were welded first from one side then from the other side. Welded panels were heat treated to T8 condition. The 50 mm regions at the both ends were cut out to remove the “run in” and “run out” regions. In this way the possibility of fatigue crack initiation at these high stress concentration regions was excluded. The panels showed low amount of distortion. The X-ray and visual examinations of the welds didn't show any significant weld imperfections other than sporadic and very small diameter pores at certain regions. The overall weld quality was very high.

2.3. Loading

Constant amplitude fatigue tests were performed on a servo-hydraulic test machine of ± 2500 kN maximum capacity. Before the test program, the load cell of the test machine was calibrated to 0.5% accuracy for the whole loading range. An initial notch of 64 mm length and 0.3 mm width was introduced in the middle of panels by electro-discharge machining (EDM) technique. With this notch, central stringers were also broken on both panels. Before the experiment, fatigue pre-cracks of about 5 mm were introduced at both sides of the machined notch. In this way, the starting crack length ($2a$) became 74 mm, which corresponds to an initial crack ratio, a_0/W of 0.1. Tests were conducted with maximum applied stress of 50 MPa at an R ratio of 0.1. Crack length measurements were done at both crack sides independently by a long distance optical microscope at every 1 mm of growth. Tests were started at a frequency of 3 Hz, at the last portion of the tests frequency reduced to first 2 Hz and then to 1 Hz to facilitate crack length recording.

For the spectrum loading fatigue tests, a modified MINI-TWIST spectrum [4] was utilized. This spectrum was basically designed for lower wing skin at the wing root and contains compressive loads. As for the desired application areas of the current test panels no severe compressive stresses expected, the negative values in the original spectrum were converted to tensile stresses simply by adding 0.7 to normalized stress values. Considering that, these tests were mainly conducted for assessing the crack retardation phenomenon in crenellated panels on the basis of performance comparison, such a modified spectrum considered to be suitable for the program objectives. Instead of creating random spectrums, one single spectrum was generated and repeatedly applied in all tests to exclude any load sequence effect. Mean flight stress, S_{mf} , was chosen as 73 MPa. Tests were performed without using anti-buckling guides on a servo-hydraulic tests machine of ± 1000 kN maximum capacity. Load values were fed to the machine with a rate of 9 load points/second, which corresponds to a frequency of 4.5 Hz. Crack length measurements were done on high resolutions photos taken independently at two crack sides at certain time intervals. Both in constant amplitude and spectrum loading fatigue tests, FCP rate, da/dN , calculations were made by the incremental polynomial fit method according to ASTM E647 appendix XI [5].

A special steel fixture, which permits the conduction of experiment with full stringer length, was designed and used in all of the tests (Figure 5).

2.4. Numerical Calculations

SIF calculations were performed by finite element method (FEM), with material constants Poisson's ratio = 0.33 and Young's Modulus = 72.4 GPa, and the assumption of straight crack front. Academic version of Solidworks software was utilized for this aim. As the number of runs necessary to get the whole profile was too high, strain energy release rate (G) method utilized, which permits very fast calculations. Considering that, for a straight crack front, $G = J$ for linear elastic case, it is possible to calculate K from J from the equation;

$$J = \frac{K_I^2}{E'} + \frac{K_{II}^2}{E'} + \frac{K_{III}^2}{2\mu} \quad [6].$$

The tests of this program basically involve mode I loadings, therefore, the K values converted from the first term of the above given equation is practically equal to average K_I values along crack front.

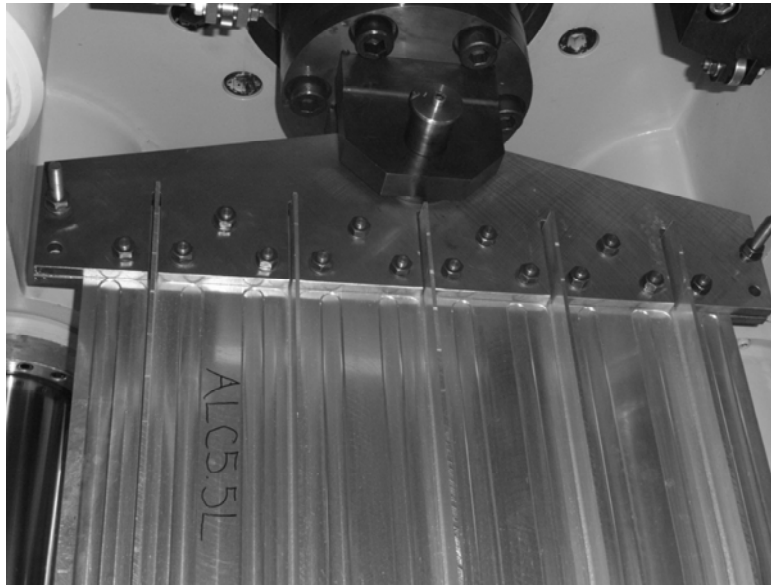


Figure 5: Loading fixture. Panels were tested with stringers extending till panel end.

3. Results and Discussion

3.1. Fatigue Crack Propagation Tests Under Constant Amplitude

Figure 6 shows the da/dN vs. a curves for the both sides of the skin crack of reference specimen tested at constant amplitude loading. The illustration at the bottom of the figure shows the corresponding panel dimension. Therefore, growth of the crack can be followed on this illustration. As can be seen, a steady state FCP rate took place till the next stringer. Then crack splitting occurred and after this point, crack propagation continued both at skin and the stringer. After the crack passed onto the stringer, FCP rate started to steeply increase for approximately 10 mm. At this point, the stringer crack (propagation of which is not shown on this graph) reached to the step on the stringer, that is, it had a length of about 10 mm. Significant crack retardation occurred at this point showing the effectiveness of the thickness step placed on the stringer. As can be realized, this event affected also the growth of the skin crack and for some 10 mm FCP rate remained constant on skin (between about 160 and 170 mm). Once the stringer crack fully passed the step and started to propagate at the thicker region of the stringer, skin crack again reacted to the behavior of the stringer crack and the FCP rate started to steeply rise at both sides of the panel (starting from app. 170 mm).

As observed during previous test programs, once the crack splitting occurs, stringer crack and the skin crack growing beyond the stringer show similar length developments. However, at the end of this test, the final crack length was about 40 mm at each stringer and about 70 mm at each side of the skin beyond the stringers. Although, the thickness step on the stringer caused some degree of crack retardation of skin crack, retardation effect on the stringer crack was still more pronounced.

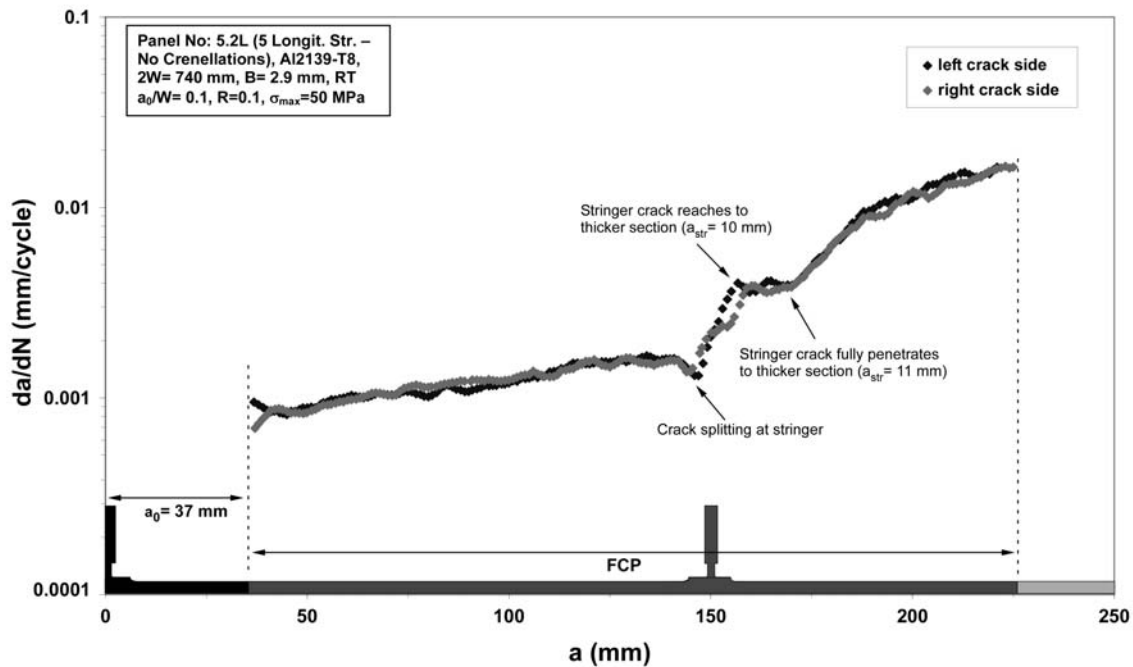


Figure 6: FCP rate vs. crack length curves of reference panel under constant amplitude loading

The da/dN vs. a curve for the crenellated panel is given in **Figure 7**. As can be seen, FCP rate showed several acceleration and deceleration on this panel contrary to **Figure 6**. By the start of the test, the FCP rates steeply decreased at both crack sides till the transition point from 1.9 mm thick region to 4.15 mm region. At this point, a minimum was experienced and after the crack passed onto the 4.15 mm thick section, rate again started to increase. This acceleration continued all along thicker region. When entering into again a 1.9 mm thick section FCP rate started to decrease. At the end of this region again acceleration was experienced, but this time with a lower slope. At stringer, crack splitting occurred and consequent crack growth took place both at skin and the stringer. After crack splitting, a rise in the FCP rate was again observed. But, similar to the case in reference specimen, the thickness step on the stringer created a retardation effect for both sides of skin cracks, which can be observed again between 160 and 170 mm on the curve. Entering of stringer crack in the thicker section triggered an acceleration in FCP rate. After that one more deceleration-acceleration loop was experienced and the experiment completed. Close to the end of the test, the stringers were broken and this also resulted in an additional rise in FCP rate. In this test the crack propagations in right and left sides were relatively asymmetric but the crack orientation remained perpendicular to the loading axis all along the test. When **Figure 7** and **Figure 2** are examined, it is clear that the governing factor for FCP rate fluctuations is the SIF profile of the panel.

Figure 8 shows the comparison of the da/dN vs. a curves for these two panels. When entering from thinner to thicker regions, FCP rate was lower for crenellated panel and vice versa. Also it can be realized that the FCP rate was lower in the crenellated panel at the 2.9 mm thick section before the stringer (between ca. 120 and 150 mm). When the overall fatigue lives of these two panels are compared it can be seen that the panel with crenellations showed approximately 65% longer life compared to the reference panel of the same weight (Figure 9).

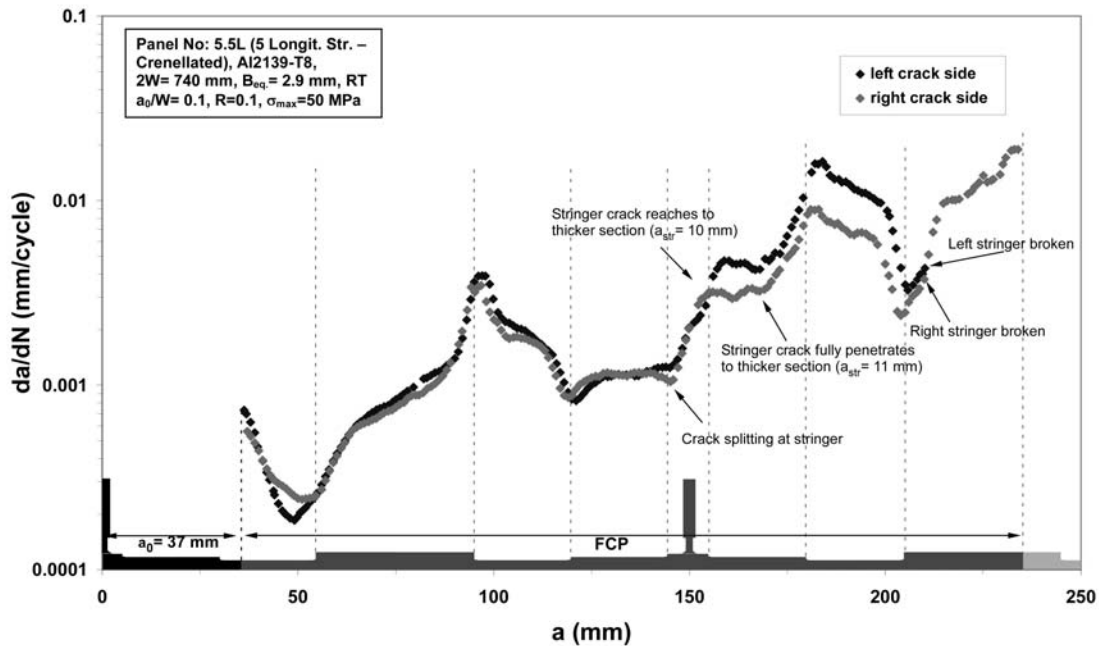


Figure 7: FCP rate vs. crack length curve of crenellated panel under constant amplitude loading

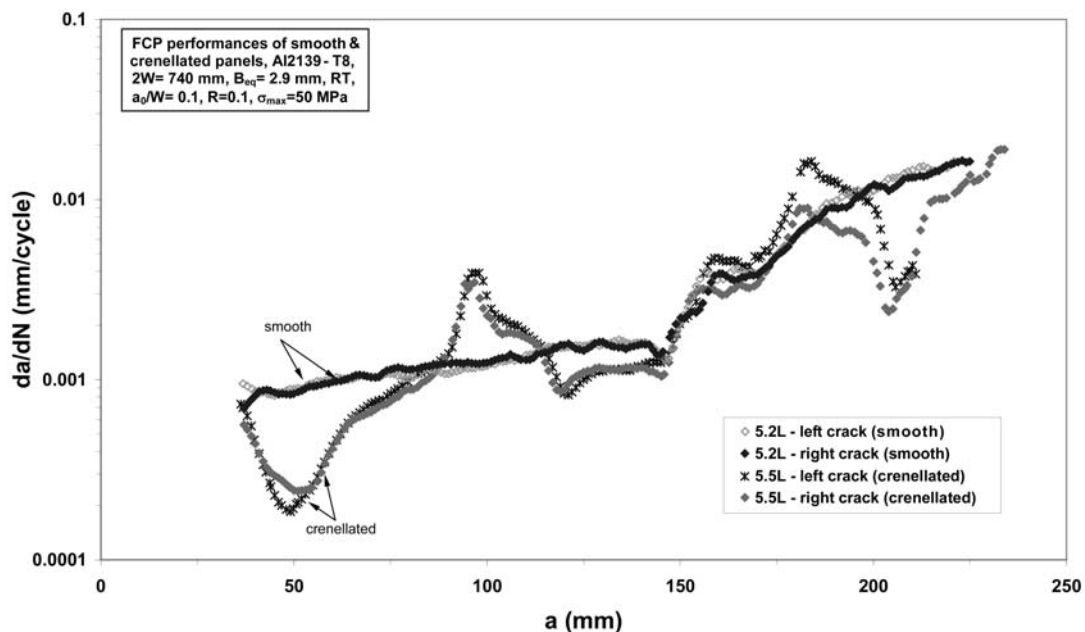


Figure 8: Comparison of FCP rate vs. crack length curves of reference and crenellated panels under constant amplitude

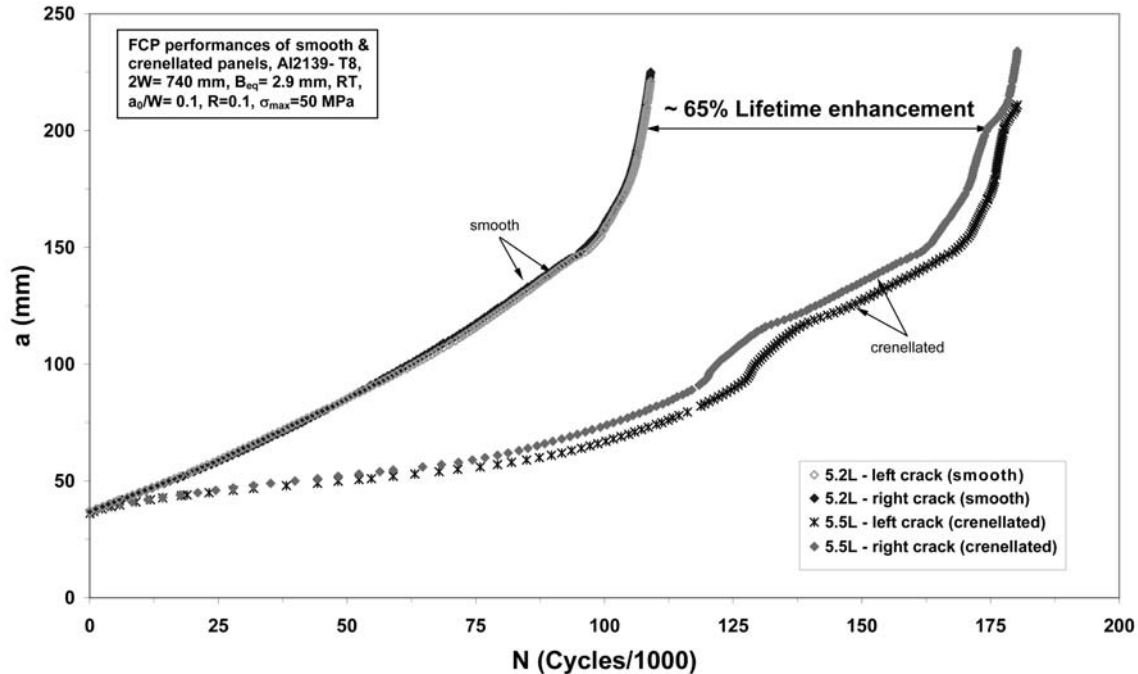


Figure 9: Comparison of a vs. N curves of reference and crenellated panels under constant amplitude loading

3.2. Fatigue Crack Propagation Tests under Spectrum Loading

The general characteristics of crack propagation under spectrum loading on the reference panel were not very different than those under constant amplitude loading (Figure 10). Again a relatively steady state propagation experienced until the stringer. But here overloads of spectrum resulted in fluctuations in the FCP rate. After reaching the stringer, FCP rate dramatically increased. At the point of stringer step, a small retardation effect was also observed. However, due to the overloads, which created small crack jumps, this effect was not clear as that was the case for constant amplitude. Crack orientation was almost perfectly perpendicular to the loading direction all along the test and a relatively symmetrical crack growth was obtained.

The da/dN vs. a curves of the crenellated panel under spectrum loading are shown in Figure 11. Here again the transition points from thinner to thicker regions resulted in retardations in FCP rate and vice versa. Crack growth on this panel was unsymmetrical. About at a length of 110 mm, right crack side showed a dramatic rise in FCP rate. At this point, the stringer on the other side of the panel was broken. Because of the loss of the stringer, the structural behavior of the panel fully changed and very high amplitude out of plane displacements started to occur.

The da/dN vs. a curves of the reference and crenellated panels are given together in Figure 12. Compared to reference panel, on the crenellated panel crack propagation rate was lower in transition location to thicker parts and higher in the transition locations to thinner sections. However, the total life gain obtained from crenellated panel increased considerably in comparison to constant amplitude loading case (Figure 13). As the shape of the curves are related to structural details, instead of using averages, curves from both crack sides are given

in this figure. It can be seen that, the total life time improvement of about 65% in the constant amplitude loading case increased up to 90-150% under spectrum loading.

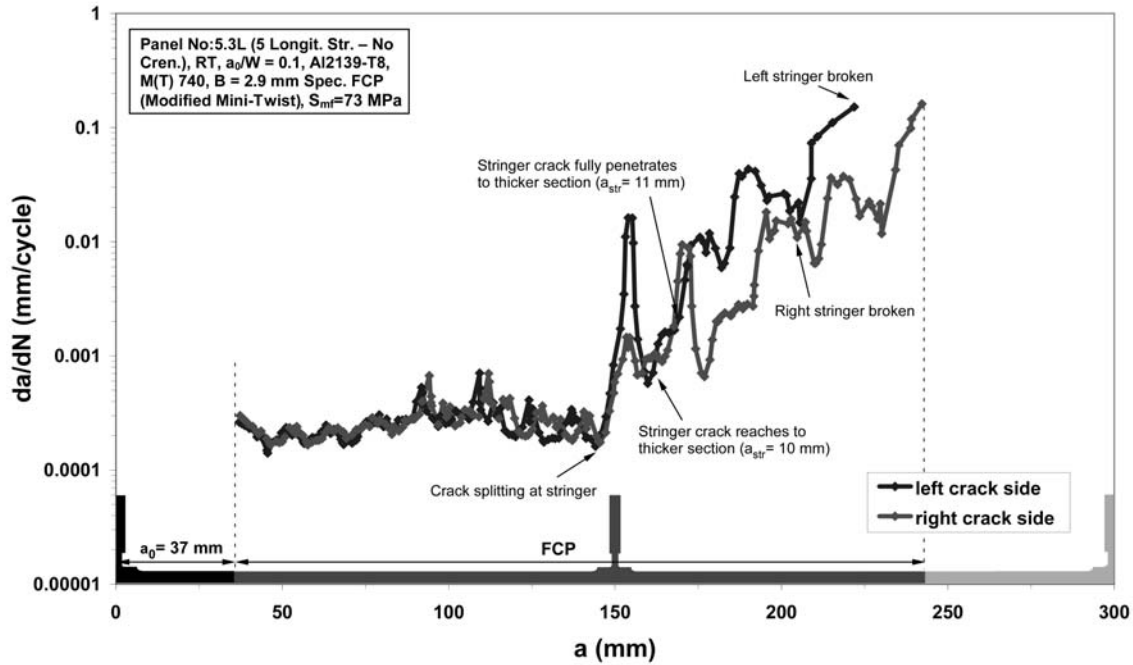


Figure 10: FCP rate vs. crack length curve of reference panel under spectrum loading

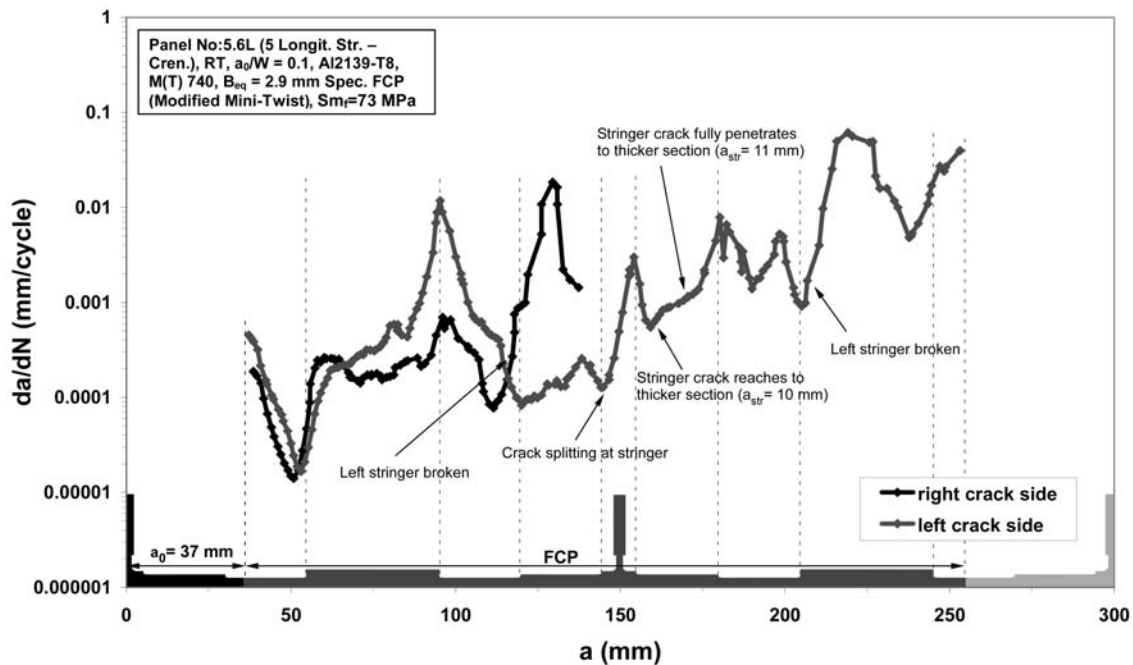


Figure 11: FCP rate vs. crack length curve of the crenellated panel under spectrum loading

Effect of tensile overloads on crack retardation effect generally attributed to the plasticity induced crack closure behind the crack tip and the compressive residual stress fields ahead of it [7, 8, 9]. Due to these phenomena, crack tip experiences a lower effective SIF range, ΔK_{eff} , compared to the pre-overload period along a certain distance. This distance is related to the

size of the plastic zone formed due to the overload. Additionally, it was shown that, the retardation effect is more pronounced in thinner specimens as the plane stress condition promotes the evolution of larger plastic zones [7, 10, 11].

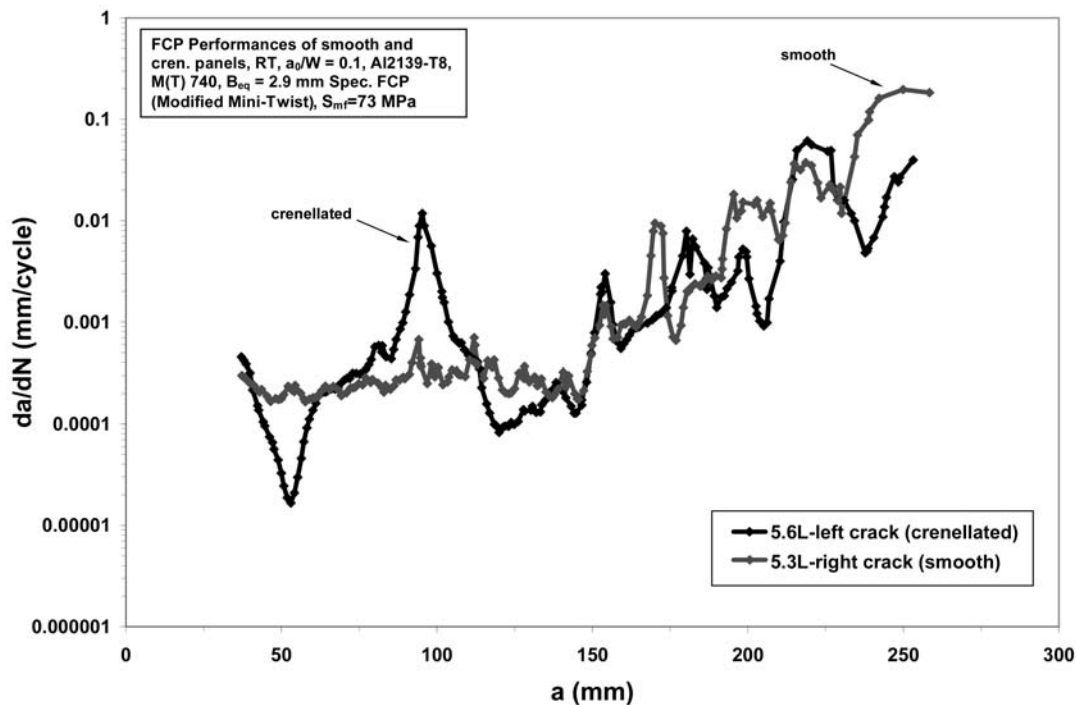


Figure 12: Comparison of FCP rate vs. crack length curves of the crenellated and reference panels under spectrum loading

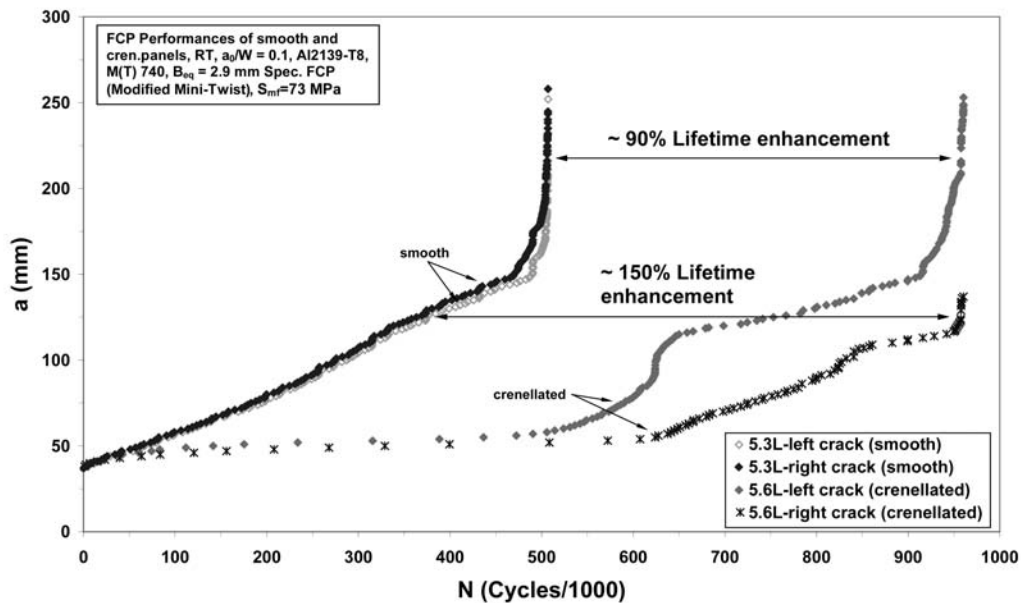


Figure 13: Comparison of a vs. N curves of reference and crenellated panels under spectrum loading

Therefore it can be expected that the thinner sections of crenellated panel utilize the retardation effect of tensile overloads more effectively. If this is the case, a reduced overload

effect may be expected at the thicker sections of the crenellated test panel with the same argumentations. Here the extent of plastic zone sizes caused by overloads must fall down compared to the reference thickness. Hence, less pronounced lifetime improvements may be expected in these regions compared to the reference panel. On the other hand, as the overall lifetime improvement is higher than that obtained in the constant amplitude case, contribution of thinner sections in life extension must have been increased. Actually, such a trend can be realized when Figures 8 and 12 examined in detail. In the case of constant amplitude loading (Figure 8), it can be seen that about 35% of the total fatigue life spent in the first 1.9 mm thick region (Cycles 0 – 67 000). After that, the crack tip entered into 4.15 mm thick area and remained in this region between the cycles ~67 000-120 000, which corresponds to about 30% of the total life. Whereas, when a vs. N curve for the spectrum loading case examined (Figure 12), it can be seen that, crack tip remained in the first 1.9 mm region for approximately 530 000 cycles (average of two crack sides) or 55% of the total fatigue life. The share of this region in the total fatigue life increased by some 20%. On the contrary, in the first 4.15 mm thick area, crack spent about 185 000 cycles or 20% of the total life which corresponds to a reduction of 10% compared to constant amplitude case. Spectrum loading extended the fatigue life in 1.9 mm region more pronouncedly, and the share of the 4.15 mm thick region in the overall fatigue life was considerably reduced.

4. Conclusion and Outlook

A new design concept for improvement of damage tolerance of laser beam welded stiffened aerospace aluminum alloy panels was investigated and significant beneficial effect was demonstrated for both constant amplitude and spectrum loading conditions for the crack growth perpendicular to the stringers.

By the help of introduction of thickness variations on skin and stringers, a new stress intensity factor distribution favoring slower overall fatigue crack propagation rates was obtained. Crenellated panels showed significantly improved fatigue life compared to reference panels under constant amplitude loading. Under spectrum loading, lifetime improvement considerably increased due to more efficient crack retardation in thinner regions of the crenellated panel.

It should be noted that, the concept of crenellations may bring a very important advantage to the metallic aerospace structures. The damage tolerance of the structures can be tailored to match the stringent design requirements. Flexibility of this new concept can serve to the development of “optimum crenellation patterns” for different parts of airframes, which in turn may result in considerable weight savings in the final structure. Further validation and certification of the concept may lead to the direct production of the desired geometries by material producers which can reduce manufacturing costs.

Furthermore, a potential success of the concept may give rise to the utilization of the design concept in other industrial applications (such as shipbuilding), where considerable differences in loading severity exist in different directions of the structures.

Acknowledgements: This work was conducted with provision of financial support of ALCAN and Technology Transfer (TT) Program of GKSS. Valuable helps of Dr. B. Petrovski and H. Tek, GKSS, during the fatigue tests are highly appreciated. First author wish to express his thanks to Dr. S. Daneshpour and D. Schnubel, GKSS, for valuable discussions during the preparation of the manuscript.

APPENDIX I**Mathematical Demonstration of Expression 3**

$$N_{ref} = \frac{2\Delta a}{C\Delta K_a^m} \quad (\text{A1})$$

$$N_{mod} = \frac{\Delta a}{C(\Delta K_a - t\Delta K_a)^m} + \frac{\Delta a}{C(\Delta K_a + t\Delta K_a)^m} \quad (\text{A2})$$

To check validity of inequality $N_{ref} < N_{mod}$ for $0 < t < 1$ (A3)

$$\frac{2a}{C\Delta K_a^m} < \frac{a}{C(\Delta K_a - t\Delta K_a)^m} + \frac{a}{C(\Delta K_a + t\Delta K_a)^m}$$

$$\frac{2a}{C\Delta K_a^m} < \frac{a}{C\Delta K_a^m} \left(\frac{1}{(1-t)^m} + \frac{1}{(1+t)^m} \right)$$

here a and ΔK are physical quantities (namely crack length and SIF range) that cannot take negative values and C is an always positive constant. Therefore inequality reduces to:

$$2 < \frac{1}{(1-t)^m} + \frac{1}{(1+t)^m} \quad (\text{A4})$$

The right side of the inequality, $f(t) = \frac{1}{(1-t)^m} + \frac{1}{(1+t)^m}$, is a continuous function of t in the open domain $(0, 1)$. The first derivative of this function with respect to t , $f'(t)$, is:

$$f'(t) = m \left(\frac{1}{(1-t)^{m+1}} - \frac{1}{(1+t)^{m+1}} \right)$$

In the given domain, denominator of the first term in parenthesis always takes a value smaller than 1 for any positive value of m . On the other hand, the denominator of the second term in parenthesis takes always greater values than 1 in the same domain for positive m . Considering that the Paris equation exponent m is positive (actually for engineering metals it takes a value between 2 and 4 [1]), the first term in parenthesis is greater and the second term is smaller than 1. Therefore, $f'(t)$ is always positive showing that $f(t)$ is an increasing function in $(0, 1)$.

At $t = 0$, the value of the $f(t)$ is:

$$f(0) = \frac{1}{1^m} + \frac{1}{1^m} = 2 \text{ for any } m.$$

As $f(0) = 2$ and $f(t)$ is an increasing function in $(0, 1)$, the inequality **A4**;

$$2 < \frac{1}{(1-t)^m} + \frac{1}{(1+t)^m} \text{ is true and the inequality } \text{A3} \text{ is satisfied for any } t \text{ in } (0, 1)$$

References

- [1] Suresh, S.(1998), *Fatigue of Materials*, Cambridge University Press, Second Edition
- [2] Kujawski, D., A new $(\Delta K + K_{max})^{0.5}$ driving force parameter for crack growth in aluminum alloys, *International Journal of Fatigue* 23 (2001), 733-740
- [3] Ehrström, J.-C., Sjoerd van der V., Arsene, S., Muzzolini, R. “Improving Damage Tolerance of Integrally Machined Panels”, *Proceedings of ICAF2005*, Hamburg, Germany
- [4] Lowak, H.; de Jonge, J.B.; Franz, j.; and Schütz, D.: “MINITWIST - A Shortened Version of TWIST.” *Laboratorium für Betriebsfestigkeit (LBF)*, Report No. TB- 146, 1979 or *National Lucht-en Ruimtevaartlaboratorium (NLR)*, NLR MP-79018U, 1979.
- [5] ASTM E647 Standard Test Method for Measurement of Fatigue Crack Growth Rates
- [6] Zehnder T. A., “Lecture Notes on Fracture Mechanics”, Available for public use at Cornell University website
http://ecommons.library.cornell.edu/bitstream/1813/3075/6/fracture_notes_2008.pdf
- [7] Sandananda K, Vasudevan AK, Holtz RL, Lee EU. “Analysis of overload effects and related phenomena”. *Int J Fatigue* 1999;21:S233–46.
- [8] McEvily, A.J., Ishihara, S., Mutoh, Y., “On the number of overload-induced delay cycles as a function of thickness”, *International Journal of Fatigue* 26 (2004), 1311-1319
- [9] Bishler, C.J., Pippin, R., „Effect of Single Overload in Ductile Metals, A Reconsideration“, *Engineering Fracture Mechanics* 74 (2007), 1344-1359
- [10] Mills, W.J. and Hertzberg, R.W., “The Effect of Sheet Thickness on Fatigue Crack Retardation in 2024-T3 Aluminum Alloy”, *Engineering Fracture Mechanics* 7 (1975), 705-711
- [11] Matsuoka, S., and Tanaka, K., “The Influence of Sheet Thickness on Delayed Retardation Phenomena in Fatigue Crack Growth in HT80 Steel and 5083 Aluminium Alloy”, *Engineering Fracture Mechanics* 13 (1980), 193-306